Journal of Alloys and Compounds 520 (2012) 89–92

Contents lists available at SciVerse ScienceDirect

Journal of Alloys and Compounds

journal homepage: www.elsevier.com/locate/jallcom

Specific features of fluorescence kinetics of BiBO:Dy^{3+} glasses

S. Klosowicz[c], W. Kuznik[a,b], M.G. Brik[b], V. Kiisk[b], S. Lange[b], I. Sildos[b], L. Jaroszewicz[c], A. Majchrowski[c], I.V. Kityk[a,*]

[a] Electrical Engineering Department, Czestochowa University of Technology, Armii Krajowej 17, Czestochowa, Poland
[b] Institute of Physics, University of Tartu, Riia 142, Tartu 51014, Estonia
[c] Institute of Applied Physics, Warsaw University Technology, Kaliskiego 2, Warsaw, Poland

ARTICLE INFO

Article history:
Received 17 November 2011
Received in revised form
16 December 2011
Accepted 19 December 2011
Available online 28 December 2011

Keywords:
Rare earth doped borates
Optical properties

ABSTRACT

Hereby we present synthesis and spectral properties dysprosium-doped BiBO glass, namely $Bi_{0.97}Dy_{0.03}B_3O_6$. We have explored UV–vis absorption, photoluminescence (PL) emission and excitation spectra as well as luminescence decay kinetics using Jasco V-570 spectrophotometer to record absorption spectrum. For measurement of PL emission spectra we have used a pulsed (pulse energy ca. 1 μJ, pulse duration 10 ns) third harmonic generation of Nd:YAG laser operating at 355 nm and 10 kHz. The experimental studies were done in a backscattering geometry. Fluorescence decay kinetics was derived from integrated time-resolved resolved spectra.

1. Introduction

The recent development of the optically operated materials is determined by a search of novel materials, which are able to vary the principal properties using appropriately varying parameters. These parameters are determined by wavelengths, power densities and frequency repetitions of the photoinduced laser beams which may be controlled during the illumination processes. The Dy^{3+} ions show promising features for the possible light emissions. In Ref. [1] the fluorescence properties of Dy^{3+} ions, with two concentrations (1.0 and 0.1 mol%), have been investigated in a variety of borate and fluoroborate glasses modified with lithium, zinc, and/or lead. The fluorescence spectra and lifetimes of $^4F_{9/2}$ level of Dy^{3+} ions in these glasses have been measured using the 457.9 nm line of argon ion laser as an excitation source. Decreasing trend in lifetimes has been observed when the glass compositions contain modifiers in the order of $LiF \rightarrow Li_2O \rightarrow ZnO \rightarrow PbO$. Decay curves for these glasses are found to be single exponential and non-exponential for 0.1 and 1.0 mol% concentrations, respectively. The non-exponential decay curves have been well fitted with the Inokuti–Hirayama (I–H) model for dipole–dipole interaction. Principal role in the borate glasses play phonon subsystem [2], contrary to the lead oxide glass–ceramic matrices [3]. And in this case the processes of photoluminescence may also be present an interest not only for the possible use in the light emitting optoelectronic devices, however, also in that case of the decay times in luminescence is a principal question which determine an applicability of the glass matrices for the fluorescent devices. In the present work we study the fluorescent features of BiB_3O_6 glass matrices for studies of Dy^{3+} ions fluorescence time decays. Additionally we will perform the Judd–Ofelt analysis and we will perform a comparison with other crystalline and glass matrices effectively varying the output fluorescence.

2. Materials and methods

2.1. Glasses preparation and doping

Molten BiBO, having high molar content of boron oxide B_2O_3, shows very large viscosity reaching 10^3 P near its temperature of crystallization [4]. This feature of BiBO makes its single crystal growth very difficult, but on the other hand it allows relatively easy glass formation. Moreover BiBO glass can be doped with high level of rare earth or transition metals ions while growth of doped BIBO single crystals leads to formation of unwanted borate phases containing dopant ions as stoichiometric components.

BiBO glass was synthesized from stoichiometric amounts of B_2O_3 (Merck Suprapur), Bi_2O_3 (Aldrich, 99.999%) and Dy_2O_3 (Aldrich 99.99%) taking into account that Dy^{+3} ions substituted bismuth ions. Bi_2O_3 and Dy_2O_3 were dried before synthesis for 24 h at 500 °C and 800 °C, respectively. To obtain glass with known composition boron oxide was molten in the first step of the synthesis in a platinum crucible. Water, that is easily absorbed by this oxide, was removed due to melting B_2O_3 and keeping it at elevated temperatures up to 1000 °C. The melt was cooled down after stopping of bubbles formation and mass of B_2O_3 was found by weighing. In the next step proper amounts of dried Bi_2O_3 and Dy_2O_3 were added to the crucible. The synthesis was carried out at 850 °C, platinum stirrer was used to make the melt homogeneous. The stirring was carried out until the melt

---

[*] Corresponding author.
E-mail addresses: ikityk@el.pcz.czest.pl, iwank74@gmail.com (I.V. Kityk).

0925-8388/$ – see front matter © 2011 Elsevier B.V. All rights reserved.
doi:10.1016/j.jallcom.2011.12.096

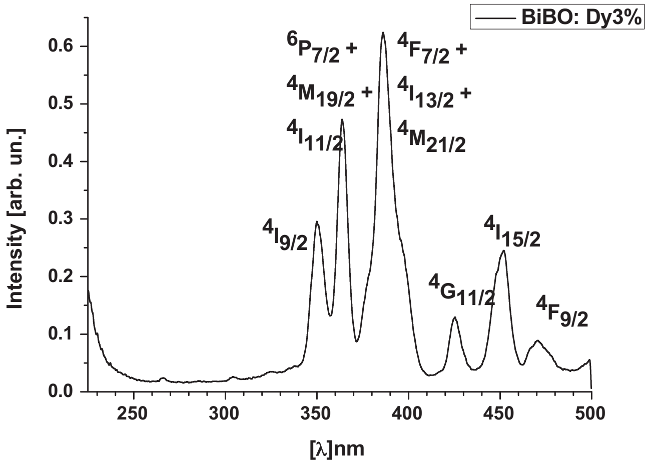

Fig. 1. Excitation spectrum of BiBO:Dy3% measured at 573 nm.

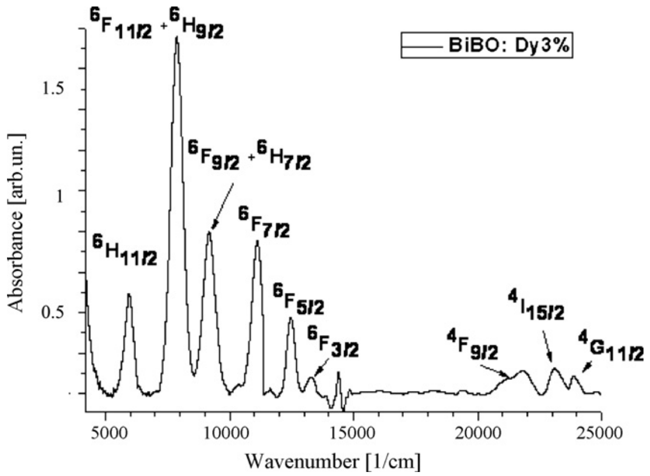

Fig. 2. Baseline-corrected absorption spectrum of BiBO:Dy3%.

became totally transparent, it took several hours at average. Finally the melt was poured onto Pt/Au 5% glass forming plate and rapidly cooled below 400 °C. Plates were cut out from formed glass with use of wire saw and polished before optical measurements.

2.2. Measurements

Photoluminescence (PL) emission and excitation spectra, luminescence decay kinetics and UV–vis absorption spectra were examined. For measurement of PL emission spectra and decay kinetics, a pulsed (pulse duration 10 ns) third harmonic generation of Nd:YAG laser operating at 355 nm and 10 kHz was used as an excitation source. The pulse energy was equal to about 1 μJ. The beam profile of the laser beam was focused in a backscattering geometry onto about 1-mm^2 spot on the surface of a sample. Spectra were recorded by a spectrograph (Andor SR-303*i*) equipped with an intensified charge coupled device (Andor DH-501) with spectral resolution up to 1 nm. This detector could be used to acquire time-resolved PL spectra with time-resolution down to 5 ns. UV–vis absorption spectrum was recorded with a Jasco V-570 spectrophotometer with spectral resolution varying within 1–2 nm. Decay kinetics was estimated by time integration of time-resolved spectra. For measurement of PL excitation spectra, a 150 W Hamamatsu xenon lamp was used in combination with a monochromator (MDR-23, spectral width 2 nm) as the tunable excitation source.

Refractive index of 1.57 and molar concentration 0.4277 mol/l were used in JO calculations. The control of scattering on the rare earth's non-homogeneities did not exceed 0.25% with respect to the signal.

3. Results and discussion

The electron absorption edge of the BiBO glass was found to be situated at approximately 390 nm. For shorter wavelengths we recorded an excitation spectrum.

The results of the measurements are presented in Fig. 1. Following the figures one can clearly see an existence of the excitation bands corresponding to excitations of $^4I_{9/2}$ level at 352 nm. More intensive are two excited spectral lines: $^5P_{7/2} + 4\,M_{19/2} + {}^4I_{11/2}$ at 368 nm and $^5F_{7/2} + {}^4I_{13/2} + {}^4M_{21/2}$ line at 388 nm. Less intensive are three excited bands at higher wavelengths: $^4G_{11/2}$ (425 nm), $^4I_{15/2}$ (452 nm) and $^4F_{9/2}$ (462 nm). The narrow half band width may indicate on the localized situation of the particular Dy^{3+} ions and an absence of an aggregation.

The absorption spectra are presented in Fig. 2. One can see that there are three very intensive spectral lines at about 800 nm (due to $^6F_{11/2} + {}^6H_{9/2}$ levels and less intensive spectral lines situated at 910 nm and 1120 nm corresponding to $^6F_{9/2} + {}^6H_{7/2}$ and $^6F_{7/2}$, respectively. The absorption spectra confirm the week broadening of the spectral lines despite substantial contribution of the electron–phonon interactions. Additional factor of such broadening may be due to specific deformations of the borate complexes in glasses.

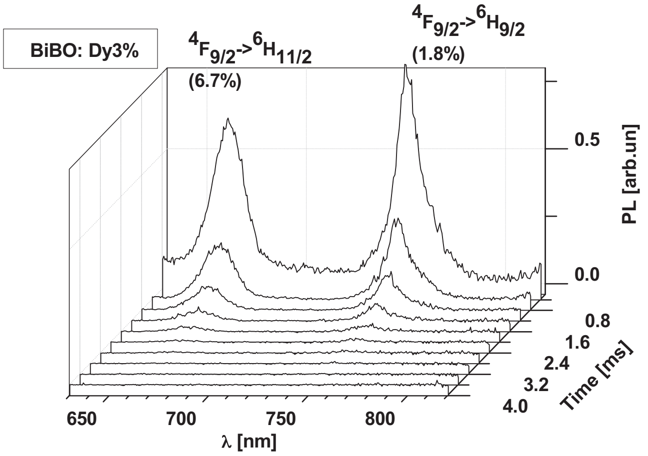

Fig. 3. Time-resolved luminescence spectrum of BiBO:Dy3% in the red region. JO branching parameters are given in brackets.

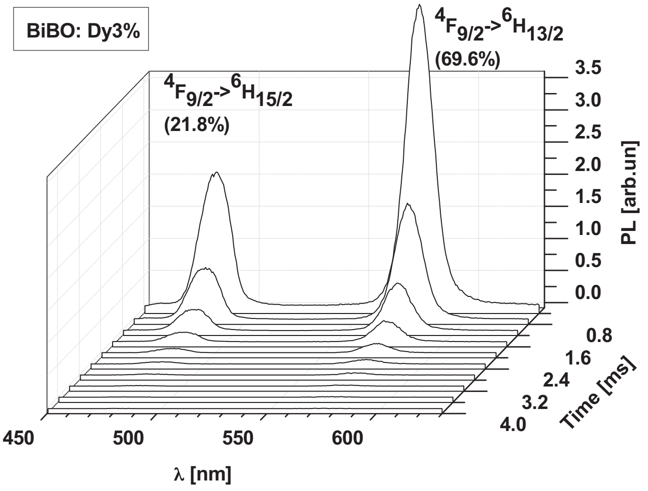

Fig. 4. Time-resolved luminescence spectrum of BiBO:Dy3% in the blue–green region. JO branching parameters are given in brackets.

The luminescence decay was examined by a time-resolved spectra measurement and subsequent integration of the emission peaks. (see Figs. 3 and 4). Following the standard logarithmic procedure (see Figs. 5 and 6) we have found that the τ is equal to 509 μs at 483 and 575 nm and 472 μs at 663 and 753 nanometer peaks.

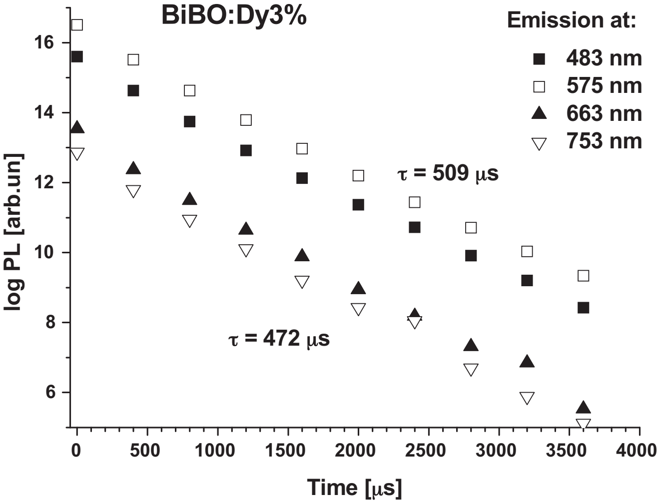

Fig. 5. BiBO:Dy3% luminescence decay curves derived from the time-resolved spectra. Lifetime in the red region is slightly shorter.

Table 1
The experimental spectral peak positions and oscillator strengths compared with calculated oscillator strengths.

Peak	Peak position [nm cm^{-1}]	Experimental OS (10^{-6})	Calculated OS (10^{-6})	
A	1684 (593)	0.63345	0.57596	$^6H_{11/2}$
B	1269 (7875)	3.19329	3.19656	$^6F_{11/2}$, $6H_{9/2}$
C	1089 (9176)	1.45268	1.45562	$^6F_{9/2}$, $^6H_{7/2}$
D	904 (11,064)	1.07542	1.08798	$^6F_{7/2}$
E	801 (12,477)	0.43251	0.49042	$^6F_{5/2}$
F	753 (13,268)	0.08994	0.09251	$^6F_{3/2}$
G	462 (21,619)	0.37935	0.08545	$^4F_{9/2}$
H	431 (23,173)	0.21329	0.22595	$^4I_{15/2}$
I	417 (23,974)	0.08262	0.0473	$^4G_{11/2}$

These observed spectral peaks are due to the transitions from the $^4F_{9/2}$ excited level to the $^6H_{15/2}$ (483 nm), $^6H_{13/2}$ (575 nm), $^6H_{11/2}$ (663 nm), and $^6H_{9/2}$ (753 nm) manifolds, correspondingly. Calculated radiative lifetime of the emitting $^4F_{9/2}$ level is 2.37 ms. The branching ratios for these transitions were found to be equal to 21.8%, 69.6%, 6.7% and 1.8%. The highest branching ratio of 69.6% is for the $^4F_{9/2}$–$^6H_{13/2}$ transition at 575 nm, indicating its highest intensity (as confirmed by the experimental spectra). The origin of the observed features is one-exponential.

The Judd–Ofelt analysis of the optical spectra was performed as described in Ref. [5] and Refs. therein. The experimental absorption spectrum parameters (frequencies and oscillator strengths) used in the analysis are presented in Table 1. A comparison with other crystalline and glass matrices is given in Table 2. One can see that the Ω_2 JP coefficient is less than for the most compared crystals and glasses and for the Ω_6 the situations seems to be opposite. Experimental lifetimes are at least fourth times shorter than the calculated ones which confirms substantial contribution of the phonon subsystem in this case. Following Fig. 5 one can see a coincidence of some relaxation times, which confirm dominant role of the glass disorder with respect to the ligand rare earth overlapping. The comparison with the lifetimes presented in Ref. [1] indicates on a more principal role in our case of the disordered potentials superimposing the local field of rare earths.

Generally the bismuth–borate matrices give higher quantum efficiency with respect to the lead–bismuth oxide glasses [14].

Table 2
Judd–Ofelt parameters and radiative lifetimes of BiBO:Dy3% compared with several literature references.

Intensity param. in [10^{-20} cm^2]	BiBO glass, this work	KPb_2Cl_5 crystal [6]	YSGG [7]	$YAl_3(BO_3)_4$ crystal [8]	$PbO–Bi_2O_3–Ga_2O_3$ glass [9]	$75NaPO_3{-}_{24}CaF_2{-}_1DyF_3$ glass [10]	ZBLAY glass [11]	$LiYF_4$ crystal [12]	MgTP glass [13]
Ω_2	2.766	6.26	0.134	1.77	6.4	3.63	3.16	2.01	7.48
Ω_4	1.311	2.45	0.726	1.05	0.5	2.03	1.67	1.34	7.15
Ω_6	1.191	0.04	1.061	1.13	1.5	1.89	2.45	2.39	7.78
Calculated lifetime $^4F_{9/2}$ [ms]	2.37	–	2.36	1.9	–	1.8	–	2.52	0.981
Exp. Lifetime $^4F_{9/2}$ [ms]	0.509	–	1.5	–	–	–	–	–	0.694

4. Conclusions

Time-resolved fluorescence kinetics together with the excitation and absorption spectra were studied for novel BiB_3O_6 glasses doped by Dy^{3+} ions. Which was embedded in the amount of 3% replacement of Bi atoms. We have found that the τ is equal to 509 μs at 483 and 575 nm and 472 μs at 663 and 753 nanometer peaks. These observed spectral peaks are due to the transitions from the $^4F_{9/2}$ (462 nm) excited level to the $^6H_{15/2}$ (483 nm), $^6H_{13/2}$ (575 nm), $^6H_{11/2}$ (663 nm), and $^6H_{9/2}$ (753 nm) manifolds, correspondingly. Calculated radiative lifetime of the emitting $^4F_{9/2}$ level is 2.37 ms. The branching ratios for these transitions are 21.8%, 69.6%, 6.7% and 1.8%. The highest branching ratio of 69.6% is for the $^4F_{9/2}$–$^6H_{13/2}$ transition at 575 nm, indicating its highest intensity (as confirmed by the experimental spectra). The origin of the observed features is one-exponential. A comparison with the experimental data has shown that the time decay kinetics is comparable with the time kinetics in typical crystalline and glass matrices and the observed discrepancies between the calculated and the experimental decay values may indicate on the main role of phonon subsystems. Additional source of the observed time kinetics may be trapping levels situated below the conduction band. These levels form resonance levels, which will substantially re-distribute the photoexcitation processes. The presented data differ from the periodic crystal due to high density of localized levels situated in the forbidden gap.

Acknowledgements

This work was partially supported by the Polish Ministry of Sciences and Higher Education, Key Project POIG. 01.03.01-14-016/08 “New Photonic Materials and their Advanced Applications” as well as by European Social Fund’s Doctoral Studies and Internationalisation Programme DoRa.

References

[1] C.K. Jayasankar, V. Venkatramu, S. Surendra Babu, P. Babu, J. Alloys Compd. 374 (2004) 22.
[2] I.V. Kityk, A. Majchrowski, Opt. Mater. 26 (2004) 33.
[3] W.A. Pisarski, J. Grobelny, R. Pisarska, G. Lisiecki, Dominiak -Dzik, W. Ryba-Romanowski, Laser Phys. 20 (2010) 649.
[4] J. Liebertz, Cryst. Growth Charact. 6 (1983) 361.
[5] A.M. El-Naggar, N.S. Alzayed, A. Majchrowski, L. Jaroszewicz, M.G. Brik, W. Kuźnik, I.V. Kityk, J. Cryst. Growth 334 (2011) 122.
[6] Y. Wang, Cryst. Res. Technol. 42 (2007) 1063.
[7] D.K. Sardar, W.M. Bradley, R.M. Yow, J.B. Gruber, B. Zandi, J. Lumin. 106 (2004) 195.
[8] K. Wang, J. Zhang, J. Li, J. Wang, H. Zhang, C. Fang, X. Zhao, Q. Zhang, J. Cryst. Growth 285 (2005) 388.
[9] Y.G. Choi, J. Heo, J. Non-Cryst. Solids 217 (1997) 199.
[10] K. Binnemans, R. Van Deun, C. Görller-Walrand, J.L. Adam, J. Non-Cryst. Solids 238 (1998) 11.
[11] Y. Tian, R. Xu, L. Hu, J. Zhang, J. Lumin. 132 (2012) 128–131.
[12] M.G. Brik, T. Ishii, A.M. Tkachuk, S.E. Ivanova, I.K. Razumova, J. Alloys Compd. 374 (2004) 63–68.
[13] D.V.R. Murthy, Opt. Mater. 32 (2010) 1112–1116.
[14] I.V. Kityk, J. Wasylak, J. Kucharski, D. Dorosz, J. Non-Cryst. Solids 297 (2002) 285.